Journal of Alloys and Compounds 580 (2013) 176–181

Contents lists available at SciVerse ScienceDirect

Journal of Alloys and Compounds

journal homepage: www.elsevier.com/locate/jalcom

Impact force for micro-detonation of striking arc machining of silicon nitrides using the Taguchi method

Baoguo Zhang *, Jianquan Wang, Xinli Tian, Xiujian Tang, Wanglong Wang, Pengxiao Wang

Science and Technology on Remanufacturing Laboratory, Academy of Armored Forces Engineering, Beijing 100072, PR China

ARTICLE INFO

Article history:
Received 26 April 2013
Received in revised form 7 May 2013
Accepted 16 May 2013
Available online 23 May 2013

Keywords:
Impact force
Micro-detonation of striking arc machining (MDSAM)
Engineering ceramics
Taguchi method

ABSTRACT

Impact force during the process of micro-detonation of striking arc machining (MDSAM) for silicon nitrides was investigated experimentally. Based on the generation principles, the orthogonal experimental design and regression analysis were employed to build the empirical model in order to understand the effects of processing parameters on impact force. It was demonstrated that for working current, working gas pressure and nozzle diameter of the micro-detonation generator, there were significant effects while for pulse width and working distance, there was hardly effect. In particular, the impact force decreased with working current and increased with working pressure and nozzle diameter. The exponential empirical model showed a good regression relationship between the processing parameters and impact force, which was verified by the experimental results. The present study could also present an important example to reveal the machining mechanism of MDSA and to provide a methodology for the control of MDSAM process.

1. Introduction

Because of their low density, superior wear, corrosion resistance, and high temperature strength, engineering ceramics like alumina, silicon nitride, and zirconia are increasingly being used in engineering application. For the engineering applications, such ceramics can be used in the production of parts, e.g., bearings, water pump seals, catalytic converters, roller followers, valves, rotors, and cutting tools [1]. However, due to the inherent hardness and brittle nature of ceramic materials, conventional techniques employing diamond grinding often lead to workpiece fracture, tool failure, low surface integrity, tool wear, low machining rate and high costs [2]. In recent years, various nontraditional machining procedures have been used in fabricating ceramic parts, including laser machining [3], laser-assisted machining [4], electrical-discharge machining [5], microwave machining [6], plasma arc cutting [7], ultrasonic machining [8], abrasive water jet machining [9], and micro-detonation of striking arc machining [10]. Among them, micro-detonation of striking arc machining (MDSAM) has been shown to be an alternative process to decrease the cost and improve efficiency.

MDSAM is a newly developed special machining technology for engineering ceramics, showing obvious advantages such as low original equipment cost, decreased operational cost, higher material removal rate and a more flexible process [11]. In combination with a NC table, MDSAM can be used for drilling, milling, turning, grooving and so on. An illustration of groove machined by MDSAM is shown in Fig. 1.

During the process of MDSAM, the ceramics is removed by the micro-detonation plasma jet which is ejecting from the nozzle of the micro-detonation generator. The micro-detonation plasma jet has the characteristics of high temperature and high impact force. When ceramics are machined with MDSAM, the material melts when the temperature in the processing region is above melting point and is thrown out from the ablation cavity by the impact force. Therefore, to study the impact force can not only reveal the machining mechanism, optimize the machining parameters and check the veracity of the calculated impact force, but can also monitor the machining process and control the machining process of MDSAM.

The Taguchi method employs a special design of orthogonal array to investigate the effects of the machining parameters through a small number of experiments and has been widely used in several engineering analysis [12]. In this paper, the Taguchi method is used to study the micro-detonation impact force. The theory of impact force is proposed, including the generation principle and the calculation model. Then, the experimental system to measure the impact force and the experimental design are given. Finally, we analyze the experiment results of the impact force and propose an empirical model for impact force.

2. Theory of impact force

2.1. Generation principle of impact force

The schematic illustration of the generation principle of the impact force during the MDSAM process is shown in Fig. 2. The

* Corresponding author.
E-mail address: zhang_baogu@126.com (B. Zhang).

0925-8388/$ - see front matter © 2013 Elsevier B.V. All rights reserved.
http://dx.doi.org/10.1016/j.jallcom.2013.05.116

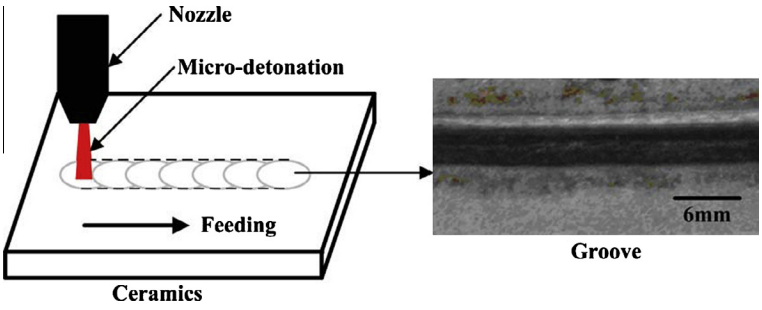

Fig. 1. Illustration of groove machined by MDSAM.

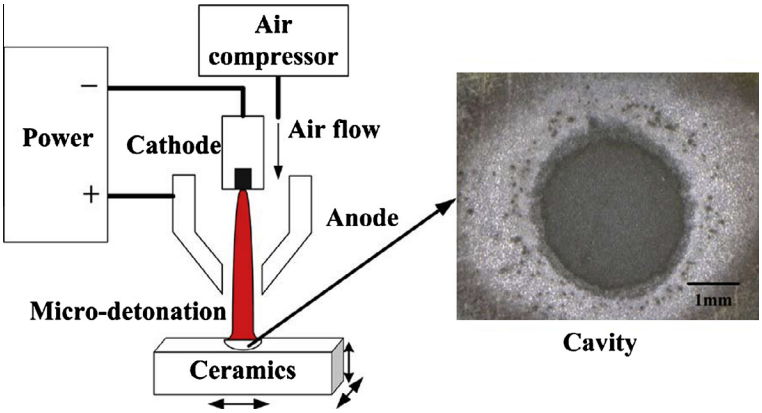

Fig. 2. The generation principle of micro-detonation impact force.

MDSAM setup consists of an air supplier, a special pulse power supply, a 3D NC table, and a micro-detonation generator.

For a MDSAM system, compressed air acts as working gas and cooling gas. The plasma jet is generated in the micro-detonation generator as the high frequency pulse voltage is supplied between two electrodes. The plasma jet expands in diameter due to the high temperature produced by the collision of high density electrons and ions. While the plasma jet passes through the nozzle, it is constricted by the combined compression effects of magnetic field, cool air flow and narrow nozzle wall. After the plasma jet bursts through from the nozzle, the plasma jet with high temperature and high pressure breaks the restraints and expands in volume. Consequently, a micro-detonation is generated and in the meantime a strong shock wave is produced. When the shock wave is applied on the workpiece, the material surface is removed by the joint action of high impact force and high temperature of micro-detonation plasma jet. After single pulse machining, a round cavity is produced, as shown in the right side of Fig. 2.

The shock wave generated by the detonation shows the typical P–t curve, as illustrated in Fig. 3. Before the arrival of the shock wave, the pressure is equal to the atmospheric pressure P_0. At the time t_a, the shock wave arrives and at the time t_b it increases to the maximum P_{max}. The pressure difference between P_{max} and P_0 is the overpressure ΔP. The pressure declines rapidly after the passing of the wave front and at time t_c it declines to P_0. Afterwards it declines continuously until a negative overpressure peak, and then gradually rises back to P_0 at the time t_d.

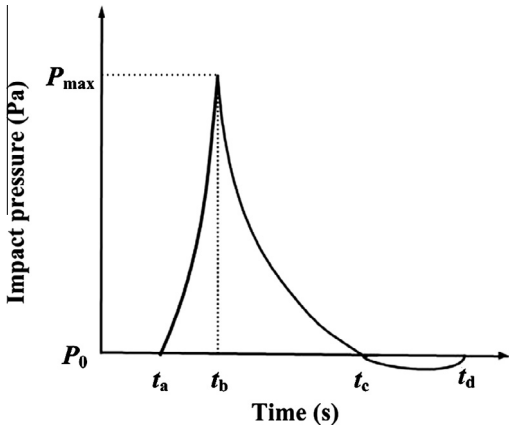

Fig. 3. P–t curve of impact pressure.

2.2. Theoretical model of impact force

The overpressure ΔP can be calculated by the following equation [13]:

$$\Delta P = \frac{7}{6}(M_s^2 - 1)P_0 \tag{1}$$

where M_s represent the mach number of the shock wave.

$$M_s = \frac{V_s}{C_0} \tag{2}$$

where V_s is the velocity of the shock wave; C_0 is the sound velocity in atmosphere, generally C_0 = 340 m/s.

According to the step change equation of shock wave in ideal gas, the shock wave velocity can be obtained:

$$V_s = M_p\sqrt{\frac{\gamma R_m T_0}{M_0}} \tag{3}$$

where M_p is the mach number of the plasma jet; γ is the adiabatic constant of gas dielectrics, γ = 1.67 for the ideal gas; R_m is the uni-

versal gas constant, R_m = 8.314 J/mol K; T_0 is the temperature of the plasma jet, which can be obtained by experiment; M_0 is the molar mass of air, M_0 = 28.959 g/mol.

In Eq. (3), the mach number of the plasma jet M_p can be calculated as following:

$$M_p = \frac{V_p}{C_0} \tag{4}$$

where V_p is the velocity of the plasma jet. V_p is obtained by the measurement experiment.

By means of test experiments on the velocity and temperature of the plasma jet, the velocity ranges from 700 m/s to 1000 m/s and the temperature ranges from 8000 K to 16,000 K. Taking a typical value as V_p = 800 m/s and T_0 = 10,000 K, Eqs. (1)–(4) are used to calculate the overpressure ΔP. The result is ΔP = 27.43 MPa. The radius of a single pulse machined cavity ranges from 1 mm to 2 mm, taking a typical value of 1.4 mm. So the impact force F_i can be obtained as the following:

$$F_i = \Delta P \cdot S = 27.43 \times 10^6 \text{ Pa} \times \pi \times (1.4 \times 10^{-3} \text{ m})^2 = 168.9 \text{ N} \tag{5}$$

Therefore, when ceramic is machined with MDSAM, the material removal is realized by the synergistic effects of the high temperature with a value of 10,000 K and the high impact force with a value of 168.9 N. This is the prominent characteristic of MDSAM.

However, there are many errors existing in the calculation results because of the hypotheses and simplification in process of calculation. In addition, the measurement of the plasma jet velocity is very difficult. To verify the correction of the theoretical calculation of the shock wave pressure and to reduce the measurement difficulty, the test on the impact force is presented in the next section.

3. Experimental procedure

3.1. Experimental setup

The schematic illustration of the experimental system to test the impact force during the MDSAM process is shown in Fig. 4, including the MDSAM system and the impact force measuring system. The impact force measuring system consists of a BK-2B unidirectional dynamometer, a signal amplifier, a PCI-8360 data acquisition card and special processing software. The practical experimental setup is shown in Fig. 5.

3.2. Material properties

This study evaluated the impact force for MDSAM of Hot Isostatically Pressed (HIPed) silicon nitride. The major mechanical properties of the material are listed in Table 1. Due to its little residual flaws and porosity, HIPed silicon nitride workpieces were more difficult to be machined compared to the reaction sintered silicon nitride workpieces [14]. The cylindrical workpiece has a diameter of 39 mm and a height of 25 mm.

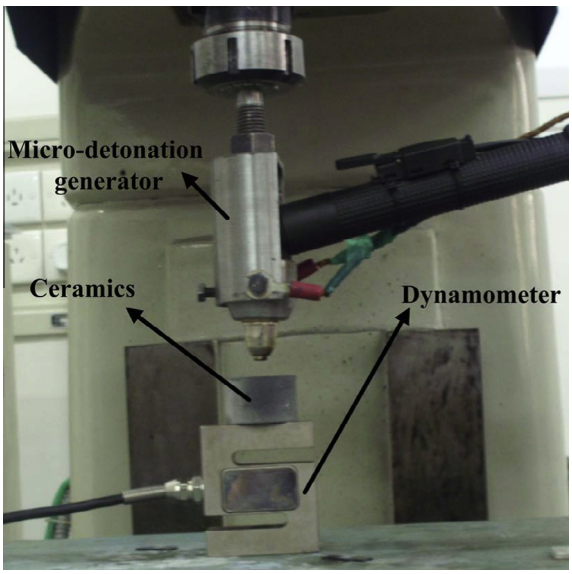

Fig. 5. The practical experimental setup used in impact force measurement.

3.3. Experimental design

In MDSAM, there are five key processing parameters to influence the impact force. They are the working current I, the working gas pressure P, the machining pulse width T, the nozzle stand-off distance L and the nozzle diameter of the micro-detonation gener-

Table 1
Material properties of HIPed silicon nitride used in the work.

Properties	Values and units
Decomposing temperature	2151 K
Density	3200 kg/m^3
Flexural strength	650 MPa
Compressive strength	3800 MPa
Elastic modulus	300 GPa
Poisson's ratio	0.28
Vickers hardness	14 GPa
Fracture toughness K_{IC}	6 MPam$^{1/2}$
Thermal conductivity	23 W/m K
Thermal expansion coefficient	2.9∗10^{-6} /K
Specific heat	660 J/Kg K

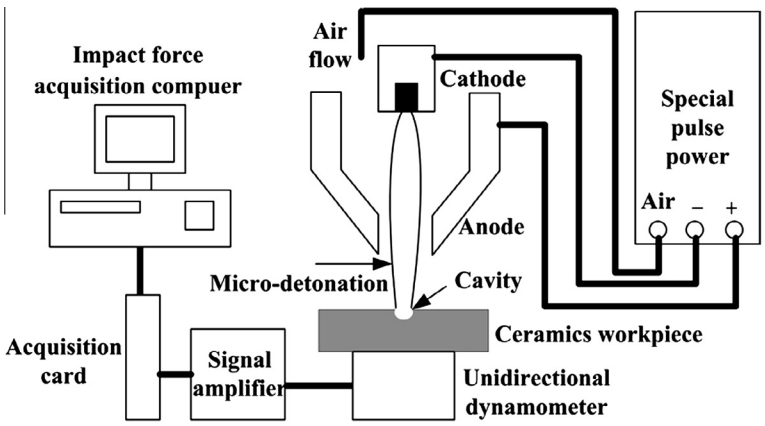

Fig. 4. Schematic illustration of the experimental system.

Table 2
Processing parameters and their levels.

Parameter	Levels				
	L1	L2	L3	L4	L5
Working current (A)	60	70	80	90	100
Gas pressure (MPa)	0.12	0.14	0.16	0.18	0.2
Pulse width (ms)	80	90	100	110	120
Nozzle stand-off distance (mm)	1	2	3	4	5
Nozzle diameter (mm)	2	2.2	2.4	2.6	2.8

ator *D*. In this research, to increase the information amount of the experiment data, the Taguchi method is employed and the orthogonal experimental design is used to study the effects of the processing parameters on the impact force. Five levels of each parameter are selected and a L_{25} (5^6) orthogonal array is selected for this work. The input processing parameters and their levels used for the experiment are listed in Table 2. To enhance accuracy of experiment, each orthogonal experiment is performed three times repeatedly.

To obtain applicable predictive quantitative relationships, it is necessary to model the processing parameters and the impact force results. In this investigation, analysis of variance of the experimental data is done to statistically evaluate the significance of each factor, and the mathematical models associated with impact force are obtained with regression method.

4. Results and discussion

The design matrix from the L25 orthogonal array based on the Taguchi method, and the experimental results of impact force are given in Table 3. The average impact force in Table 3 is 169.4 N, which is very close to the theoretical calculation result of 168.9 N by Eq. (5), validated that the theoretical model of Eqs. (1)–(4).

4.1. ANOVA analysis of the results

ANOVA analysis of the experiment results is carried out to determine the significant processing parameters. The contribution of the processing parameter is defined as significant if the calculated *F* ratio values exceed $F_{0.05}(4,4)$. The results of ANOVA of impact force obtained from the L_{25} array based on Taguchi method are presented in Table 4. It can be seen from Table 4 that the working current, working gas pressure and nozzle diameter have significant contribution. The significance sequence of influence degree of parameters on impact force is shown as follows: nozzle diameter, working current, and working gas pressure.

Table 3
Orthogonal array L25 and experiment results of impact force.

No.	*I* (A)	*P* (MPa)	*T* (ms)	*L* (mm)	*D* (mm0	*F* (N)
1	60	0.12	80	1	2	163
2	60	0.14	90	2	2.2	166
3	60	0.16	100	3	2.4	173
4	60	0.18	110	4	2.6	189
5	60	0.2	120	5	2.8	198
6	70	0.12	100	2	2.6	177
7	70	0.14	110	3	2.8	182
8	70	0.16	120	4	2	168
9	70	0.18	80	5	2.2	167
10	70	0.2	90	1	2.4	179
11	80	0.12	120	3	2.2	159
12	80	0.14	80	4	2.4	168
13	80	0.16	90	5	2.6	177
14	80	0.18	100	1	2.8	185
15	80	0.2	110	2	2	171
16	90	0.12	90	4	2.8	170
17	90	0.14	100	5	2	149
18	90	0.16	110	1	2.2	161
19	90	0.18	120	2	2.4	165
20	90	0.2	80	3	2.6	172
21	100	0.12	110	5	2.4	144
22	100	0.14	120	1	2.6	165
23	100	0.16	80	2	2.8	173
24	100	0.18	90	3	2	155
25	100	0.2	100	4	2.2	159

Table 4
ANOVA analysis of impact force results.

Parameters	Sum of squares	Degree of freedom	*F* ratio	$F_{0.05}(4,4)$	Significance
I	1222	4	14.632	6.39	*
P	538	4	6.442		*
T	58	4	0.694		
L	19.2	4	0.23		
D	1608	4	19.254		*
Error	83.52	4			

4.2. Effect of processing parameters on impact force

The average values of impact force at each level for the five processing parameters are calculated to find out the parameter effects. Effects of processing parameters on impact force are shown in Fig. 6.

Fig. 6a with the working current of 60, 70, 80, 90 and 100 ms, the impact force varies obviously. From the results, it can be seen that the impact force decreases with the increment of the working current. In MDSAM, the machining energy is outputted by micro-detonation. The increment of the working current will lead to the expansion of micro-detonation. Therefore, the inner pressure of micro-detonation will decrease, causing the reduction of the impact force.

Fig. 6b shows the impact force variations with gas pressure of 0.12, 0.14, 0.16, 0.18 and 0.2 MPa. As the working gas pressure increases, the higher the impact force is that can be obtained. The micro-detonation is generated by the ionization of working gas. The increment of gas pressure will reinforce the ionization degree of working gas and result in the increasing of impact force.

Fig. 6c shows the impact force variations with the machining pulse width of 80, 90, 100, 110 and 120 ms. With the increase of the working pulse width, the impact force changes less and has no distinct relationship with the pulse width. A longer pulse width will increase the processing duration, causing the augment of material removal, but has little influences on the impact force.

Fig. 6d shows the impact force variations with the working distance of 1, 2, 3, 4 and 5 mm. As the working distance increases, the impact force changes in a very small range, illustrating the working distance has less effect on the impact force. However, if the distance is too long, the impact force will be reduced. Because the plasma jet has a length limit of about 10 mm, the impact effect will be decreased gradually while the working distance approaches 10 mm.

Fig. 6e shows the influences of the nozzle diameter of the micro-detonation generator on the impact force. With the nozzle diameter of 2.0, 2.2, 2.4, 2.6 and 2.8 mm, the impact force is considered. When the nozzle diameter increases, the impact force becomes bigger. This is because the expansion of nozzle diameter will increase the gas flow under a certain fixed working gas pressure. A bigger flow enhances the ionization degree of working gas, leading to a higher inner pressure of plasma jet.

4.3. Empirical model of impact force

Processing experiment results in Table 3 with a multiple linear regression method, the following regression result can be obtained:

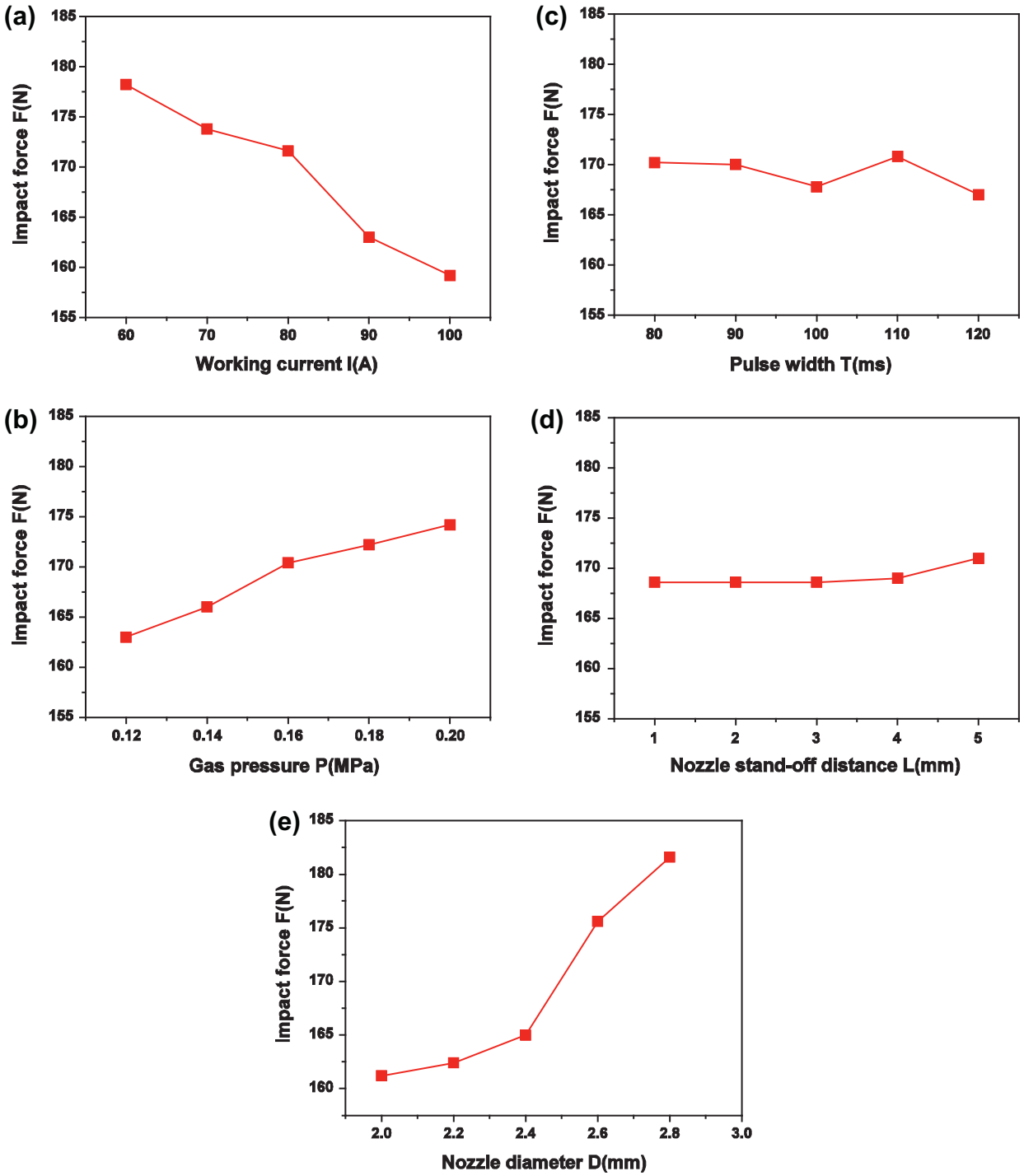

Fig. 6. The effects of processing parameters on impact force: (a) working current, (b) gas pressure, (c) pulse width, (d) nozzle stand-off distance and (e) nozzle diameter.

$$y = 2.5953 - 0.2205x_1 + 0.1507x_2 + 0.018x_3 - 0.0117x_4 + 0.3727x_5 \quad (6)$$

where y is impact force at logarithmic scale; x_1, x_2, x_3, x_4 and x_5 is the working current, gas pressure, working distance, pulse width, nozzle stand-off distance and nozzle diameter at logarithmic scale, respectively.

Therefore, the empirical model of the impact force F_i is:

$$F_i = 393.8I^{-0.2205}P^{0.1507}T^{0.018}L^{-0.0117}D^{0.3727} \quad (7)$$

From Eq. (7), it can be seen that the nozzle diameter has the greatest influence on the impact force with the coefficient of 0.3727, followed by the working gas pressure with a coefficient of −0.2205, and then the working gas pressure with a coefficient of 0.1507. For the coefficients of pulse width and working distance are so small that the influences of the two parameters can be neglected.

To test of the significance of the regression model, F statistics are used. The F statistics can be given as follows:

$$F = \frac{\mathrm{ESS}/k}{\mathrm{RSS}/(n-k-1)} : F(k, n-k-1) \quad (8)$$

Table 5
Results of the ANOVA assessment for the regression model of impact force.

Source	Sum of squares	Degree of freedom	F ratio	$F_{0.01}(5,19)$	Adjusted R^2
Model	0.020467	5	30.193	4.17	0.85879
Error	0.002576	19			
Sum	0.023043	24			

Table 6
Results of the ANOVA assessment for the regression coefficients.

Source	Coefficient	t Value	$t_{0.01}(19)$
Constant	2.5953	26.46	2.5395
Working current	−0.2205	−7.42	
Gas pressure	0.1507	5.07	
Pulse width	0.018	0.48	
Working distance	−0.0117	−1.24	
Nozzle diameter	0.3727	8.27	

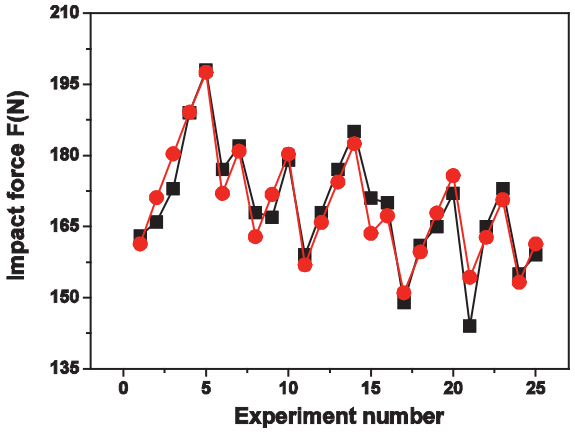

Fig. 7. Comparison of the experimental results and calculation results of the impact force.

where n is the number of experiment, ESS is the error sum of squares, RSS is the regression sum of squares, and k is the number of variations. At the preset confidence level, if $F > F(k, n-k-1)$, the regression equation can be considered credible.

Using the experiment results in Table 3, the test results are listed in Table 5.

From Table 5, we can find that with the preset confidence level of 0.01, the F value of the regression equation is greater than $F_{0.01}(5,19)$. The adjusted R^2 with the value of 0.85879 shows the goodness of fit. The results show that the impact force has a highly significant regression relationship with the parameters and the empirical model is proper.

The t statistic is employed to test the regression coefficients. At the preset confidence level, if the t value is bigger than listing value, the regression coefficients can be considered significant. The test results are listed in Table 6.

From Table 6, we can find that the t values of constant, working current, working gas pressure and nozzle diameter are bigger than the critical value of $t_{0.01}(19)$, illustrating these four parameters are significant for the regression model and cannot be neglected. The t values of pulse width and nozzle stand-off distance are smaller than critical. Therefore, the two parameters must be eliminated. Using the impact force data in Table 3, the new model with the other three parameters can be changed to the following equation:

$$F_i = 423I^{-0.2205}P^{0.1507}D^{0.3727} \quad (9)$$

The validity of the impact force model Eq. (9) is verified by comparison with the data in Table 3. The result is shown in Fig. 7. From Fig. 7 we can find that the calculation results by Eq. (9) is very close to the experimental results in Table 3. The biggest error with the value of 6.67% occurs at the No. 21 group experiment. The results indicate that the impact force empirical model is in good agreement with the experimental results. Eq. (9) can be used to predict and control the impact force.

5. Conclusions

(1) The plasma jet in the micro-detonation generator is compressed by the magnetic force, cool air flow and the mechanical compression of the nozzle wall. When it ejects from the nozzle, a micro-detonation is generated and a strong shock wave is produced. The shock wave is applied on the ceramics surface and the impact force is generated.
(2) In the processing parameters of MDSAM, working current, working gas pressure and the diameter of the micro-generator nozzle have significant influence on the impact force while the pulse width and working distance have minor influences on impact force. The impact force has an inverse relationship with the working current and direct proportion with the gas pressure and the nozzle diameter.
(3) By means of the Taguchi method and ANOVA analysis, the empirical model of the impact force is established. Significant tests of regression model and regression coefficients show that the model is credible to predict and calculate the impact force. The model can be used to control the process of MDSAM.

Acknowledgments

This work was supported by the National Natural Science Foundation of China (No. 51075399), the Twelfth Five-Year National Defense Pre-research Projects (No.51318020210), and Beijing Natural Science Foundation (No. 3132022).

References

[1] A.N. Samant, N.B. Dahotre, Adv. Eng. Mater. 10 (2008) 978–981.
[2] C. Barnes, P. Shrotriya, P. Molian, Int. J. Mach. Tools Manuf. 47 (2007) 1864–1874.
[3] A.N. Samant, N.B.J. Dahotre, Eur. Ceram. Soc. 29 (2009) 969–993.
[4] B. Yang, X. Shen, S. Lei, Int. J. Mach. Tools Manuf. 49 (2009) 344–350.
[5] N. Mohri, Y. Fukuzawa, T. Tani, N. Saito, K. Furutani, CIRP. Ann–Manuf. Tech. 45 (1996) 201–204.
[6] E. Jerby, V. Dikhtyar, O. Aktushev, U. Grosglick, Science 298 (2002) 587–589.
[7] W.J. Xu, J.C. Fang, Y.S.J. Lu, Mater. Process. Technol. 129 (2002) 152–156.
[8] Z.C. Li, L.W. Cai, Z.J. Pei, C. Treadwell, Int. J. Mach. Tools Manuf. 46 (2006) 1469–1477.
[9] P. Gudimetla, J. Wang, W.J. Wong, Mater. Process. Technol. 128 (2002) 123–129.
[10] X.L. Tian, J.F. Yang, C. Liu, B.G. Zhang, F. Guo, A.B. Yu, Int. J. Adv. Manuf. Technol. 48 (2010) 529–536.
[11] B.G. Zhang, X.L. Tian, A.B. Yu, X.J. Tang, J.Q. Wang, Int. J. Adv. Manuf. Technol. 64 (2013) 1565–1573.
[12] R.J. Ji, Y.H. Liu, Y.Z. Zhang, B.P. Cai, H. Li, J.M. Ma, Int. J. Adv. Manuf. Technol. 51 (2010) 195–204.
[13] H.T. Cui, Q.M. Liu, Exp. Meas. Fluid. Mech. 18 (2004) 92–96.
[14] J. Lee, S. Lim, D. Shin, H. Sohn, J.J. Kim, Laser. Micro/Nanoeng. 4 (2009) 207–211.